

PLUG-IN VEHICLE CONTROL STRATEGY: FROM GLOBAL OPTIMIZATION TO REAL-TIME APPLICATION

Dominik Karbowski
Argonne National Laboratory

Aymeric Rousseau, Sylvain Pagerit, Phillip Sharer
Argonne National Laboratory

Abstract

Plug-in hybrid electric vehicles (PHEVs) have demonstrated the potential to significantly increase fuel economy. However, the overall efficiency of the powertrain system of any Hybrid Electric Vehicle (HEV) depends on the vehicle-level control strategy. To optimize the energy flow, a global optimization algorithm, based on the Bellman principle, was used to generate the most efficient operating conditions for a parallel pre-transmission hybrid and a specific driving cycle. Several driving cycles were analyzed, each of them repeated a number of times to assess the impact of driving distance. The engine, electric machine, and transmission operating modes were then used to generate a rule-based control strategy in PSAT, Argonne's vehicle system modeling software.

Keywords: Plug-in Hybrid, Parallel HEVs, Hybrid Strategy, Modeling, Simulation

1 Introduction

Hybrid Electrical Vehicles (HEVs) are undergoing extensive research and development because of their potential for high efficiency and low emissions. Their controls, like those for any other vehicle, have to maximize fuel economy, which, in this case, is highly dependent on the power allocation between the fuel converters (engine and fuel cell) and the energy storage system(s). A global optimization algorithm on the powertrain flows has been developed on the basis of the Bellman optimality principle and applied to fuel cell HEVs [1]. This algorithm has been modified and enhanced to be able to manage the issues introduced by Plug-in HEV (PHEV) specificities. The optimization results are used to isolate control patterns, both dependent and independent of the cycle characteristics in order to develop real-time control strategies in Simulink/Stateflow. These controllers are then implemented in Argonne National Laboratory's Powertrain System Analysis Toolkit (PSAT) to validate their performances.

PSAT [2, 3], developed with MATLAB/Simulink, is a vehicle-modeling package used to simulate performance and fuel economy. It allows one to realistically estimate the wheel torque needed to achieve a desired speed by sending commands to different components, such as throttle position for the engine, displacement for the clutch, gear number for the transmission, or mechanical braking for the wheels. In this way, we can model a driver who follows a predefined speed cycle. Moreover, as components in PSAT react to commands realistically, we can employ advanced component models, take into account transient effects (e.g., engine starting, clutch engagement/disengagement, or shifting), and develop realistic control strategies. Finally, by using test data measured at Argonne's Advanced Powertrain Research Facility, PSAT has been shown to predict the fuel economy of several hybrid vehicles within 5% on the combined cycle. PSAT is the primary vehicle simulation package used to support the U.S. Department of Energy's (DOE's) FreedomCAR R&D activities.

PHEVs introduce increased complexity because of the length of the driving cycles or the battery state-of-charge (SOC) range considered. In addition, the selection of a parallel HEV configuration with a multi-gear transmission adds a degree of freedom, in comparison to the initial fuel cell hybrid vehicle with the gear ratio selection. In this study, we will assess the impact of the distance and characteristics of the drive cycle on the optimum component control. Finally, the global optimization results will then be used to develop a StateFlow control strategy in PSAT.

2 Vehicle Assumptions

Table 1 lists the main characteristics of the simulated midsize car. The components selected are the ones that have been implemented in Argonne’s Mobile Advanced Automotive Testbed (MATT). MATT [4] is a rolling chassis used to evaluate component technology in a vehicle system context. The control strategy developed on the basis of the optimization results will ultimately be implemented and tested on hardware.

Table 1: Vehicle Main Specifications

Component	Specifications
Engine	2.2 L, 100 kW Ford Duratec
Electric machine	30 kW Continuous UQM
Battery	Li-ion – Saft VL41M
Transmission	5-speed manual transmission Ratio: [3.42, 2.14, 1.45, 1.03, 0.77]
Frontal Area	2.244 m ²
Final Drive Ratio	3.8
Drag Coefficient	0.315
Rolling Resist.	0.008 (plus speed related term)
Wheel radius	0.3175 m

As shown in Figure 1, the configuration selected is a pre-transmission parallel hybrid, very similar to the one used in the DaimlerChrysler Sprinter Van [5].

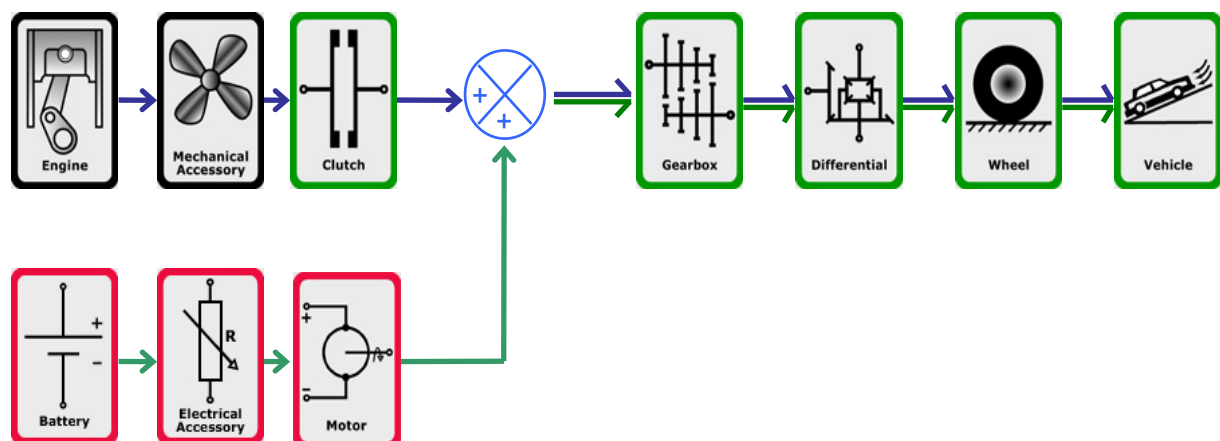


Figure 1: Configuration Selected – Pre-Transmission Parallel HEV

3 Global Optimization

3.1 Static Power Flow Modeling

Because the number of computations is critical in optimization algorithms, simplified models and assumptions must be used. For this reason, static component models can be used for backward simulation of the HEV, as illustrated in Figure 2.

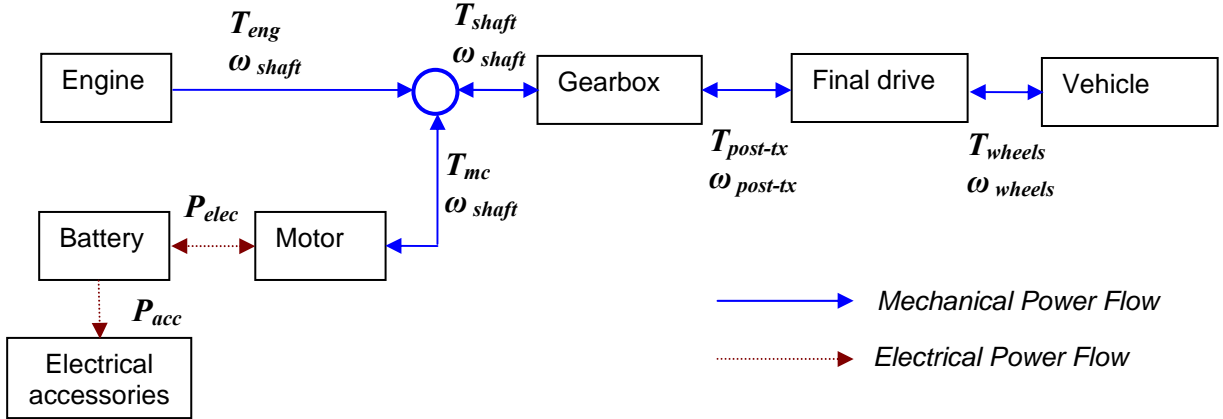


Figure 2: Static Vehicle Model

For this phase, the component models used are based on look-up tables, including engine fuel rate, as well as electric machine, transmission, and gear ratio torque losses. A specific battery model has been developed to take into account the specificities of PHEVs [6].

3.2 Algorithm Principle

3.2.1 Generic Algorithm — Bellman Principle

The battery state-of-charge (SOC) is the key parameter in the algorithm, as it determines the level of charging and discharging. It is sampled and can take m values: $SOC \in [SOC_1, \dots, SOC_k, \dots, SOC_m]$.

The command is defined by the engine torque and the gear number. The motor torque and the battery power are defined by the engine torque demand because the motor is assumed to provide the difference between the demand torque and the command engine torque.

Beginning from the end, the cycle is followed backward. At each time step t , all the combinations of commands that comply with each component constraints are taken into account. For each possible SOC_k and combination of commands $(T_{eng}^{(p)}, gear_q)$, the instantaneous loss $L_{inst}^{(p,q,k)}$ and the implied SOC at time $t+1$, $SOC_{\psi(p,q,k)}$, are calculated. For each SOC_k at time t , the optimal path to the end is given by the command $(T_{eng}^{(p)}, gear_q)$ that minimizes the cumulated losses:

$J_k(t) = \min_{j \in \{1, k', l', m\}} (L_{inst}^{(p,q,k)} + J_{\psi(p,q,k)}(t+1))$. Figure 3 illustrates the algorithm at step t . Finally, the command, the implied $SOC_{\psi(p,q,k)}$, and the corresponding $J_k(t)$ are stored, in order to be used in computation at time $t-1$ and in the post-processing.

The path finally chosen between t and $t+1$ is not necessarily the optimal path between t and $t+1$ that would achieve instantaneous optimization. The algorithm indeed considers the entire drive cycle. Once the algorithm reaches the initial step, a post-processing algorithm collects the data previously stored at each step and builds the optimal command on the basis of the predetermined initial and final SOC values.

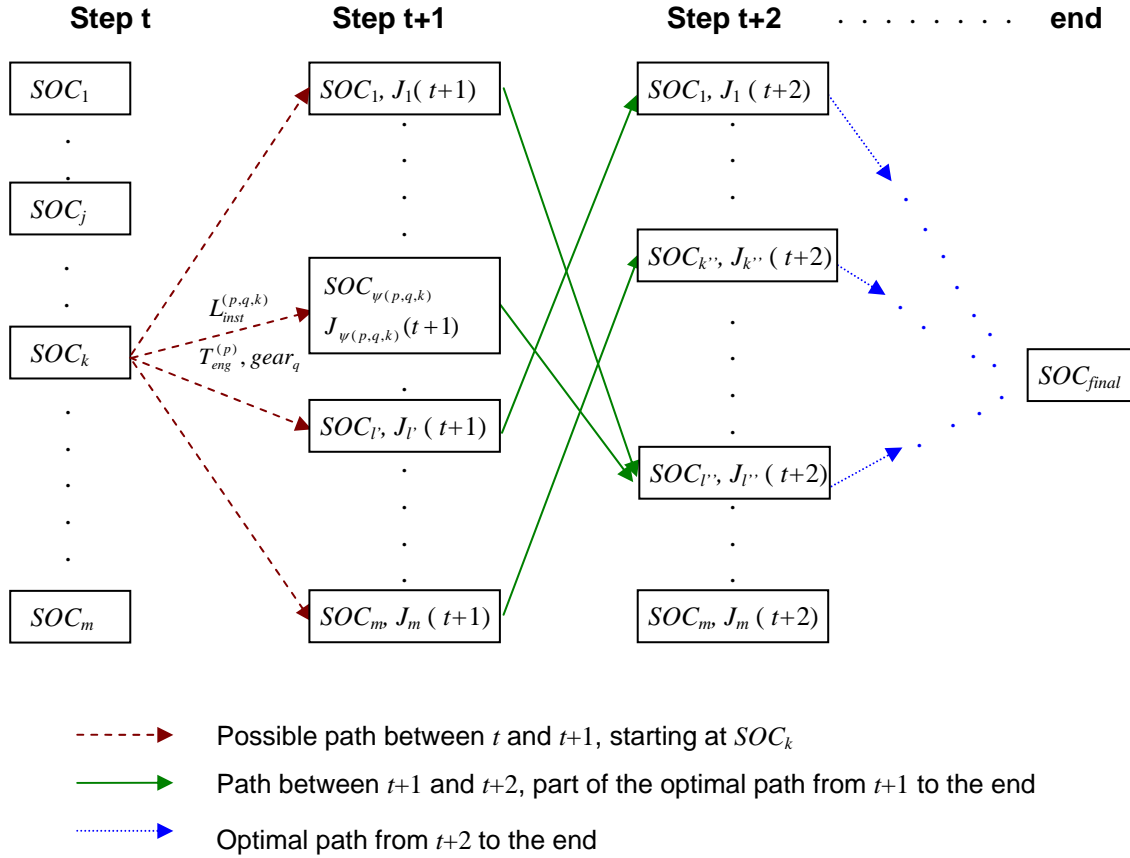


Figure 3: Global Optimization Process

3.2.2 Nature of the optimization

The global optimization aims at minimizing the cumulative energy loss throughout the cycle:

$$\min_{\{possible\ commands\}} \left(\int_{cycle} L_{inst}(t) dt \right).$$

The losses of the main components are taken into account with $L_{inst}(t) = L_{inst}^{eng}(t) + L_{inst}^{motor}(t) + L_{inst}^{battery}(t)$.

When regenerative braking energy is used to charge the battery, $L_{inst}(t) = 0$ is used to recuperate as much energy as possible. However, this free energy cannot be differentiated from the energy from the grid once it is stored in the battery and is therefore included in $L_{inst}(t)$ when being discharged.

The losses due to other components are indirectly accounted for in $L_{inst}(t)$, because higher losses in those components are likely to require more fuel and electricity and, thus, more losses at the engine and /or the battery and motor.

The algorithm outputs the control strategy that will yield the best energy efficiency, not necessarily the best fuel economy – even though the differences of efficiency between the engine and the electrical system are such that it is usually the case. In the present optimization, we considered that one joule of fuel energy is equivalent to one joule of electricity from the grid, but other quantifying coefficients can be used to compare these two sources of energy: actual cost (gasoline costs 2.5 c/MJ [\$3/gal], electricity costs 2.2 c/MJ [8 c/kWh]), environmental cost (obtained by a well-to-pump analysis, for example), and emissions, among others.

3.2.3 Main Parameters and Methodology

One of the main algorithm constraints is the initial and final battery SOC, which were respectively selected to be 90% and 30%. In addition, to evaluate the impact of driving cycles, the New European Driving Cycle (NEDC), Urban Driving Dynamometer Schedule (UDDS), and Japan 1015 were selected. Each cycle has been repeated several times to assess the impact of distance on the control.

3.3 Results

3.3.1 Blended versus Electric Only Control Strategy

When considering PHEVs, one major issue is whether to use the battery as much as possible before operating in charge-sustaining mode (electric-only strategy) or use the engine throughout the driving cycle (blending strategy). Figure 4 shows the battery SOC as a function of different driving cycles. For illustration, an example of electric-only control based on the default simulation control is provided from the simulation. When analyzing the optimization results, one notices that the lower SOC value is only reached at the end of the cycle. The algorithm clearly favors the blending control strategy.

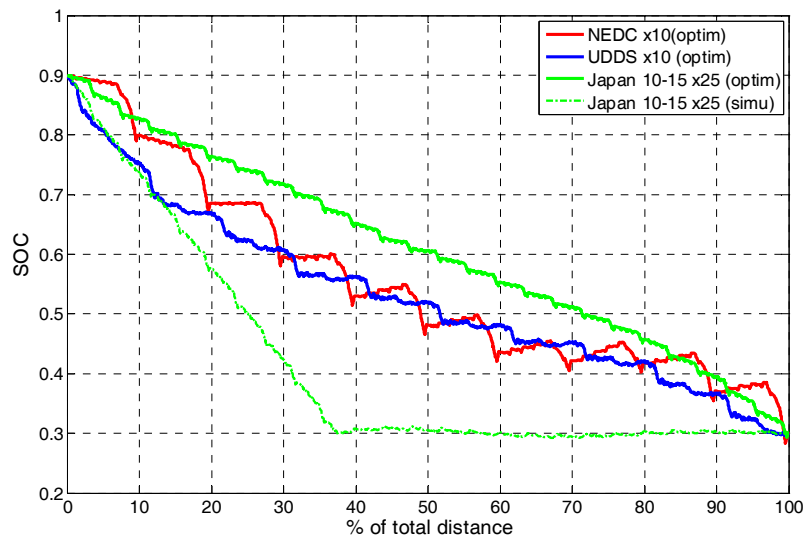


Figure 4: Evolution of Battery SOC for Different Driving Cycles

3.3.2 Evolution of Engine ON Frequency

When considering charge-sustaining HEVs, the optimization results provide similar behaviors when the same cycle is repeated successively because of the low energy available from the battery. PHEVs add another degree of freedom. As a consequence, one may ask whether the optimum behavior is

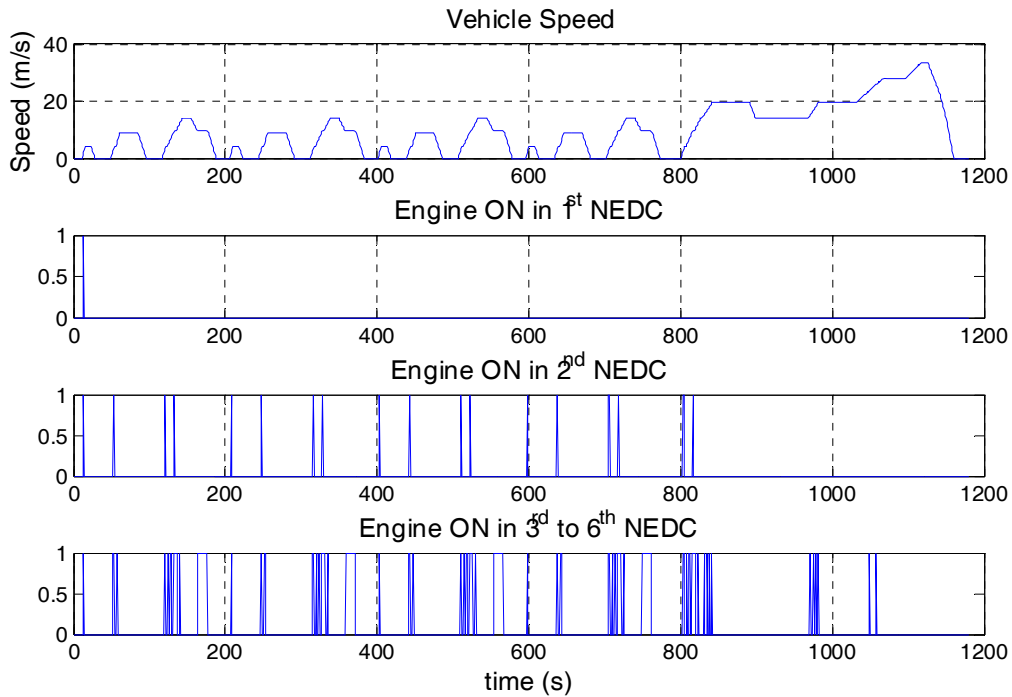


Figure 5: Evolution of Engine ON Frequency

similar from one cycle to another. Figure 5 shows the evolution of the engine ON when the NEDC is repeated 6 times. Note that the first cycle is performed in electric-only mode. During the second cycle, the engine is started more often to finally start at the same times for the remaining cycles (3 to 6).

One main reason to delay the engine start is to maximize regenerative braking energy. Because of the high initial SOC, the maximum charging power of the battery is limited, as shown in Figure 6. After the first NEDC, the regenerative braking increases to reach its maximum value during the third cycle. From there, lowering the SOC for regenerative braking purposes is not an issue anymore.

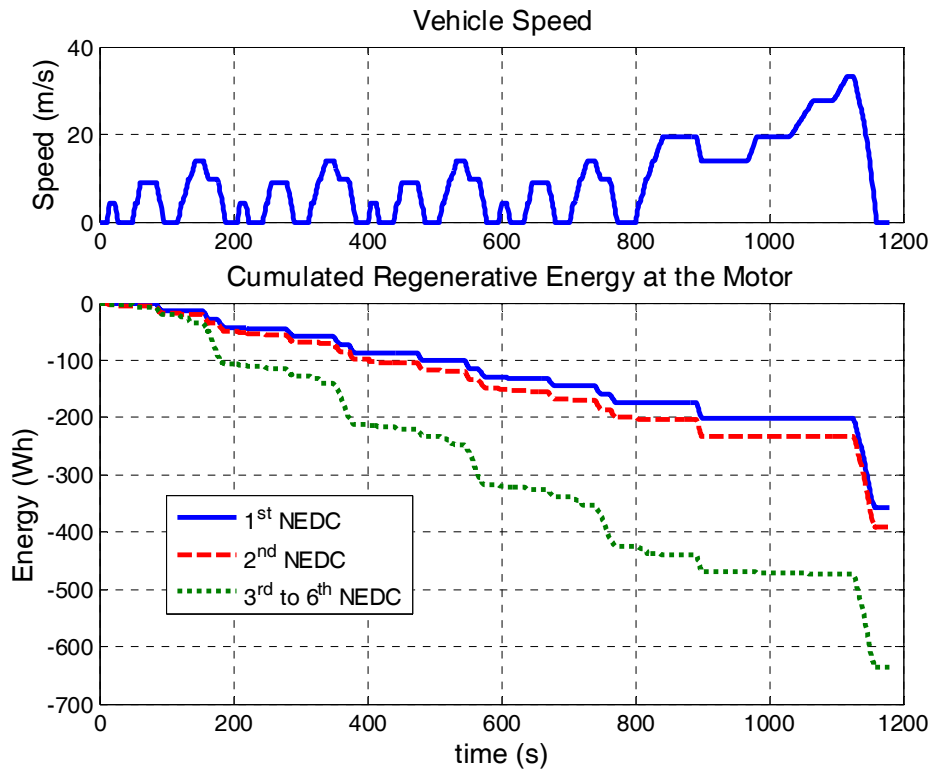


Figure 6: Regenerative Energy Increases

3.3.3 Battery Charging from Engine

One of the most difficult questions with HEVs is whether or not to recharge the battery from the engine and when. Indeed, the additional roundtrip efficiencies from the engine to the battery have to be considered, including the electric machine. The increased energy from the engine should then still be higher than the losses to charge the battery and then to provide the energy back to the powertrain. Figure 7 shows the engine power used to recharge the battery. Note that when the SOC is lower, the engine is used to recharge the battery at a maximum power of 10 kW on the NEDC. The algorithm only decided to use the engine in its best efficiency area.

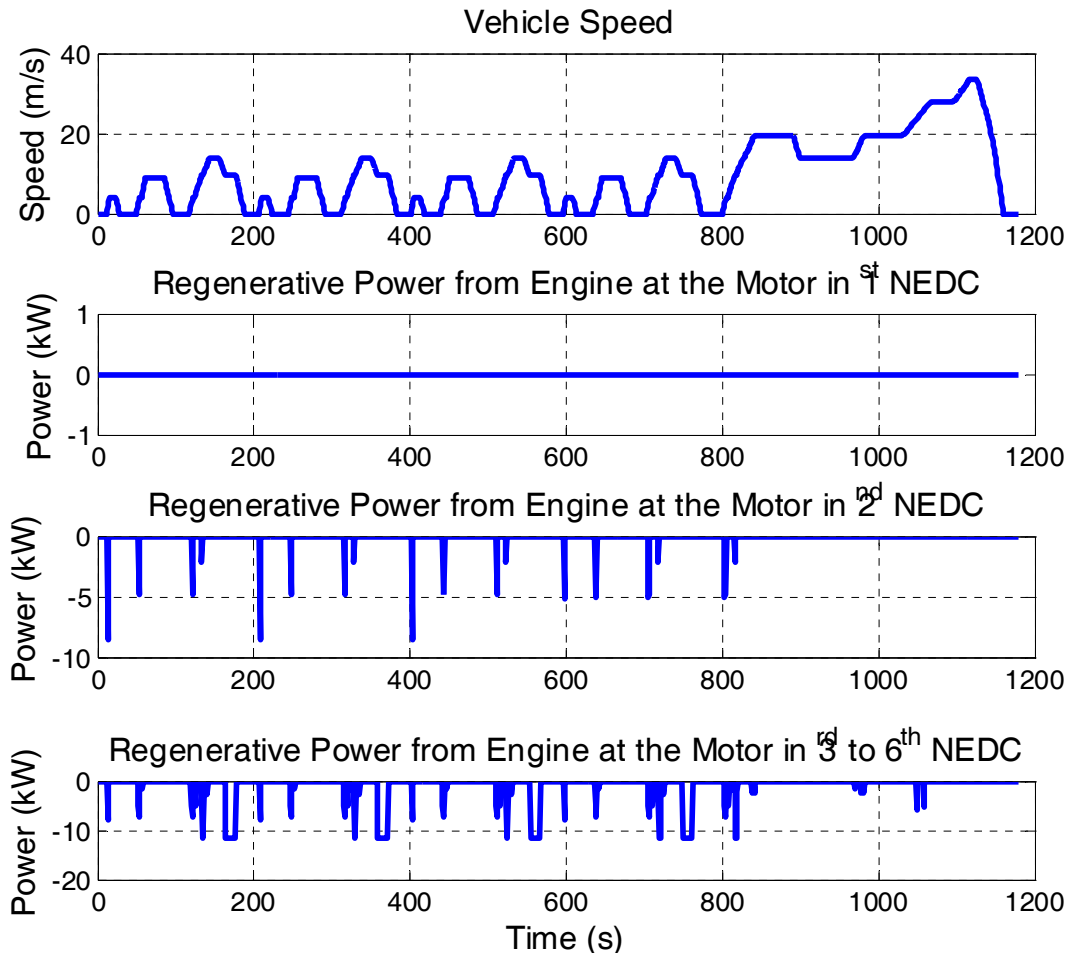


Figure 7: Battery Charging from Engine

3.3.4 Minimum SOC Only Reached at the End

Figure 8 shows the electrical energy consumed during each cycle of a $10 \times$ NEDC run. When the first two cycles are mostly performed in electric mode (EV), note that the electrical contribution decreases until the 8th cycle, when it finally increases again. As shown in Figure 4, the final SOC value is only reached at the end of the cycle. This behavior can be explained by the increased battery losses at low SOC as a result of an increased current because of the lower voltage. Consequently, it is important to know the length of the driving cycle to operate at low SOC as little as possible.

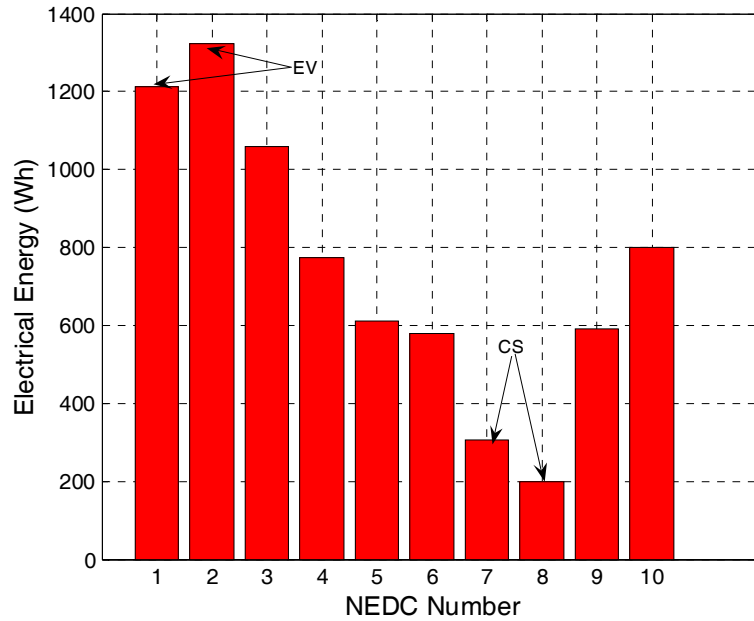


Figure 8: Electrical Energy Consumed during Each NEDC

3.3.5 Influence of Driving Cycle

Figure 9 shows the cumulative engine ON time for several driving cycles. To compare similar distances, different numbers of cycles have been used. For a lower distance, the cumulative engine ON time varies from one cycle to another and increases with the aggressiveness of the cycle — the Japan1015 being the least aggressive and the NEDC the most. However, when the distance increases, the difference becomes negligible.

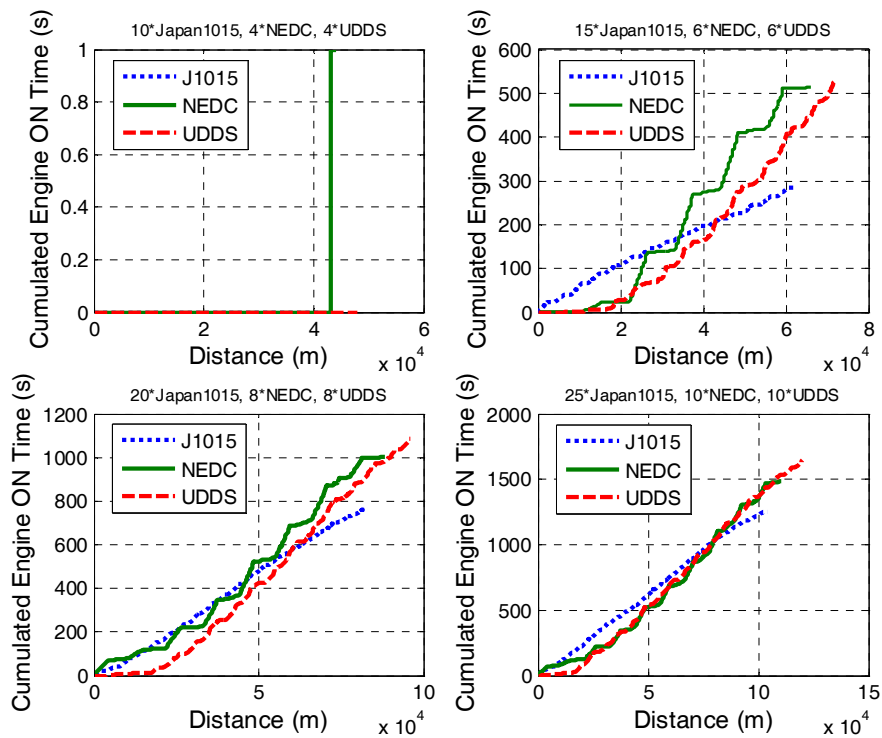


Figure 9: Influence of Driving Cycle on Engine ON Time – $10 \times$ Japan1015, $4 \times$ NEDC, $4 \times$ UDDS

4 Real-Time Controller

4.1 PSAT Default Control Strategy

The adopted control strategy is based on two modes shown in Figure 10:

1. Charge-depleting (CD) mode: corresponds to the discharge of the battery from its maximum SOC value (battery charged) to a lower threshold higher than the minimal SOC (battery discharged). During this mode, the controller uses the electric energy that was previously taken from the grid, as well as from the engine.
2. Charge-sustaining (CS) mode: corresponds to a PHEV0 control; as the SOC is too low, no electric energy taken from the grid is available, but some energy can still be recovered from regenerative braking and used afterwards at selected moments.

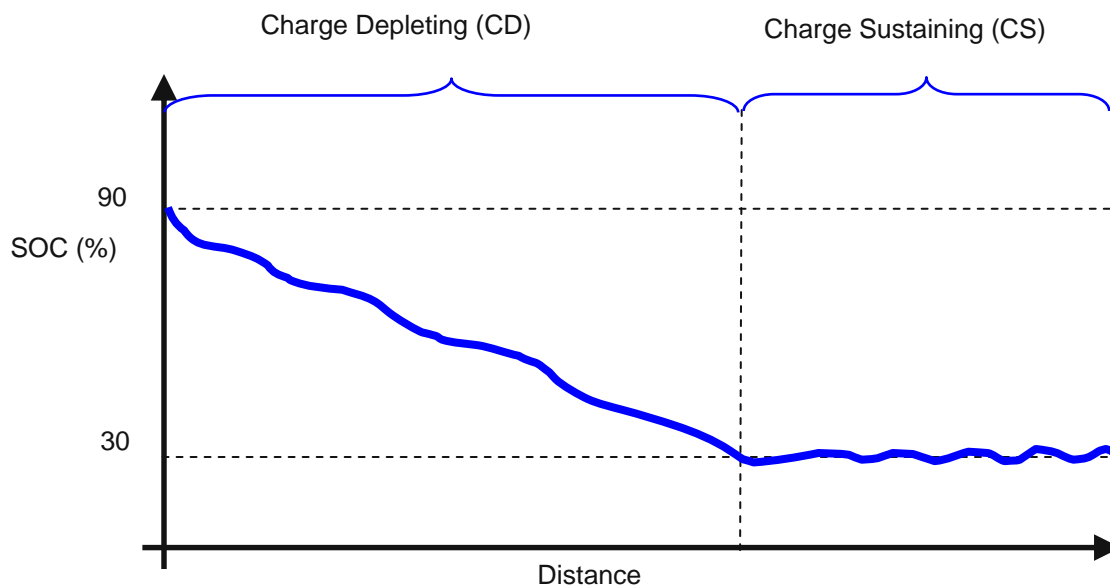


Figure 10: Global Optimization Process

4.2 Comparison with Global Optimization

Figure 11 compares the engine and motor energy as well as their sum. The total energy from the simulation is similar to the optimization, which validates both vehicle models. As the default control strategy in PSAT favors the electrical consumption, the motor is almost exclusively used at the beginning of the trip, with the engine taking over toward the end of the simulation. Once the engine starts, the vehicle operates in CS mode. The electrical energy decreases because of the electrical accessory load. The results from the optimization, on the contrary, show a more balanced repartition between the electrical and the thermal energies throughout the trip.

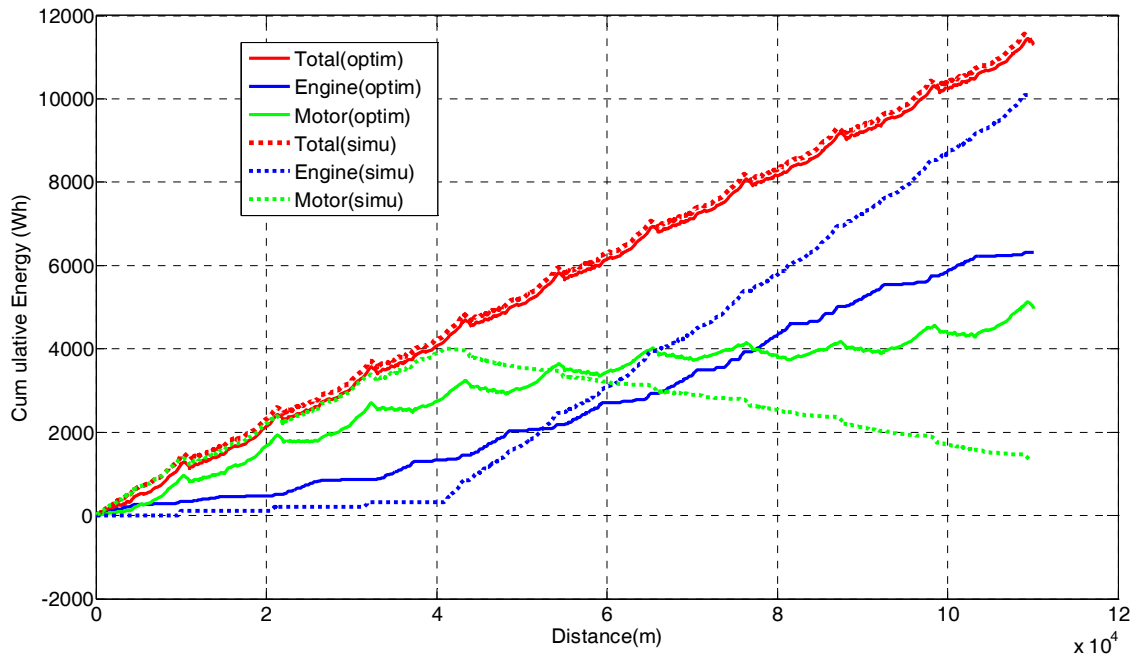


Figure 11: Engine and Motor Output Energy Comparison – NEDC $\times 10$

Figure 12 shows the input energies from both the engine and the battery. The final total energy from the default simulation control is almost 60% higher than that from the optimization algorithm.

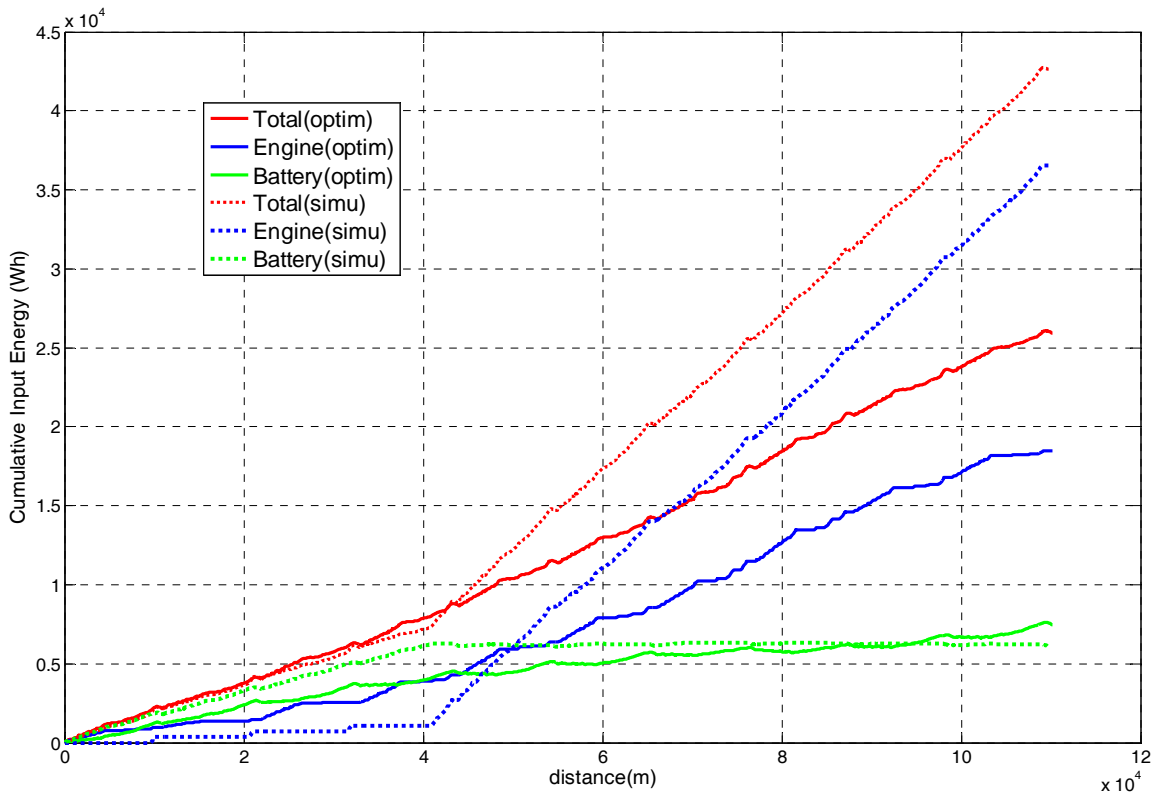


Figure 12: Engine and Battery Input Energy Comparison – NEDC $\times 10$

The main reason for the difference in energy use is because of the operating conditions of the engine. As shown in Figure 13, during the optimization, the engine is only operated around its best efficiency area. Because the battery SOC decreases rapidly for the default simulation case, the powertrain is forced to operate under CS conditions, and the engine is operated in a larger operating area.

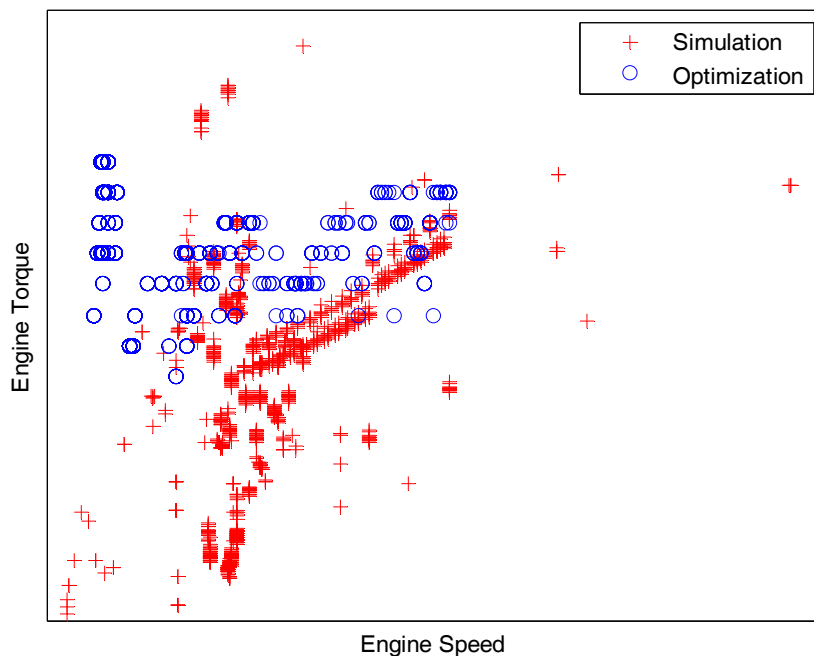


Figure 13: Comparison of Engine Operating Conditions – NEDC \times 10

5 Conclusions

When optimizing a CS HEV, the main parameter influencing the control strategy is the driving cycle — repeating the same driving cycles will not alter the control strategy patterns. For PHEVs, distance also needs to be carefully considered. The share between the electrical and thermal energy is consequently more difficult to determine because the optimum control will change on the basis of distance. Although we want to achieve the lowest available SOC at the end of the cycle, we also want to avoid running the vehicle in CS mode at lower SOC values with high battery losses. Knowing the destination will become an even more important factor for PHEVs.

After the battery has been recharged, the first part of the trip should be completed in electric mode to quickly lower the SOC to maximize regenerative braking energy. Once this is achieved, the engine ON pattern is similar for the remainder of the trip. The engine should be used during high acceleration events and vehicle speeds. To increase overall powertrain efficiency, the engine should only be used at its best efficiency, which would result in the recharging of the battery. Toward the end of the driving cycle, less time needs to be spent at low SOC.

To conclude, developing optimized real-time control strategies for PHEVs is more challenging than for CS HEVs because of distance implications. Future control strategy studies will use the optimization results as a reference. The controller will be based on average vehicle miles traveled (VMT) to focus the tuning on the distance that most people drive. Finally, the vehicle control strategy will be implemented in MATT to control hardware to take into account engine cold start and emissions.

References

- [1] Pagerit, S.; Rousseau, A.; and Sharer, P., “*Global Optimization to Real Time Control of HEV Power Flow: Example of a Fuel Cell Hybrid Vehicle*,” EVS 21, April 2005.
- [2] Argonne National Laboratory, PSAT (Powertrain Systems Analysis Toolkit), <http://www.transportation.anl.gov/>.
- [3] Rousseau, A.; Sharer, P.; and Besnier, F., “*Feasibility of Reusable Vehicle Modeling: Application to Hybrid Vehicles*,” SAE paper 2004-01-1618, SAE World Congress, Detroit, March 2004. <http://www.eere.energy.gov/vehiclesandfuels>.
- [4] Shidore, N.; Bohn, T.; Duoba, M.; Loshe-Bush, H.; and Pasquier, M., “*Innovative Approach to Vary Degree of Hybridization for Advanced Powertrain Testing using a Single Motor*,” EVS22, October 2006.
- [5] Graham, B., “*Plug-in Hybrid Electric Vehicle, A Market Transformation Challenge: the DaimlerChrysler/EPRI Sprinter Van PHEV Program*,” EVS21, April 2005.
- [6] Sharer, P.; Rousseau, A.; Nelson, P.; and Pagerit, S., “*Vehicle Simulation Results for Plug-in HEV Battery Requirements*,” EVS22, October 2006.

Authors



Dominik Karbowski, Research Aide, Argonne National Laboratory, 9700 South Cass Avenue, Argonne, IL 60439-4815, USA, dominik.karbowski@mines-paris.org

Dominik Karbowski received a Master degree in Science and Executive Engineering from the Ecole des Mines de Paris, France, in 2006. Focused on energy, his thesis is based on global optimization applied to plug-in hybrid vehicles.



Aymeric Rousseau, Research Engineer, Argonne National Laboratory, 9700 South Cass Avenue, Argonne, IL 60439-4815, USA, arousseau@anl.gov

Aymeric Rousseau is head of the Advanced Powertrain Vehicles Modeling Department at Argonne National Laboratory. He received his engineering diploma at the Industrial System Engineering School in La Rochelle, France, in 1997.



Sylvain Pagerit, Research Engineer, Argonne National Laboratory, 9700 South Cass Avenue, Argonne, IL 60439-4815, USA, spagerit@anl.gov

Sylvain Pagerit received a Master of Science in Industrial Engineering from the Ecole des Mines de Nantes, France, in 2000 as well as a Master of Science in Electrical Engineering from the Georgia Institute of Technology, Atlanta, in 2001.



Phillip Sharer, Research Engineer, Argonne National Laboratory, 9700 South Cass Avenue, Argonne, IL 60439-4815, USA, psharer@anl.gov

Phillip Sharer is Systems Analysis Engineer at Argonne National Laboratory. He received a Master of Science in Engineering from Purdue University Calumet in 2002. He has over five years of experience modeling hybrid electric vehicles using PSAT at Argonne National Laboratory.